Reentry Attitude Tracking Control for Hypersonic Vehicle with Reaction Control Systems via Improved Model Predictive Control Approach

Kai Liu[1, 2], Zheng Hou[2, *], Zhiyong She[2] and Jian Guo[2]

Abstract: This paper studies the reentry attitude tracking control problem for hypersonic vehicles (HSV) equipped with reaction control systems (RCS) and aerodynamic surfaces. The attitude dynamical model of the hypersonic vehicles is established, and the simplified longitudinal and lateral dynamic models are obtained, respectively. Then, the compound control allocation strategy is provided and the model predictive controller is designed for the pitch channel. Furthermore, considering the complicated jet interaction effect of HSV during RCS is working, an improved model predictive control approach is presented by introducing the online parameter estimation of the jet interaction coefficient for dealing with the uncertainty and disturbance. Moreover, considering the strong coupling effect between the yaw channel and roll channel, a coupled model predictive controller is designed by introducing the feedback of sideslip angle into the roll control channel to eliminate the coupling effect. Finally, the comparison simulations using the classical control method, MPC and IMPC approach are given to demonstrate the effectiveness and efficiency of the presented IMPC scheme.

Keywords: Hypersonic vehicle, reentry attitude control, mode predictive control, jet interference factor, reaction control systems.

1 Introduction

Hypersonic vehicles (HSV) have huge value in both military and civil applications due to their high speed, strong reliability and good penetration capability [Feng and Zhou (2017); Greg (2006); Liu (2011); Weingarten (1993); Zhou, Liu and She (2015)], which have become a hot research topic in the aerospace area during the last few decades. The HSV will dramatically reduce the operational cost of space missions because of the fact that they can be used repeatedly by recovering and reusing after each launch mission.

Due to the wide flight envelop, large uncertainties and unknown external disturbances, the attitude control design of HSV, particularly in the reentry phase [Cheng, Tang, Wang

[1] School of Aeronautics and Astronautics, Dalian University of Technology, Dalian, 116024, China.

[2] Key Laboratory of Advanced Technology for Aerospace Vehicles, Dalian, 116024, China.

[3] Beijing Institute of Aerospace Technology, Beijing, 100074, China.

* Corresponding Author: Zheng Hou. Email: hou_zhengyq@163.com.

Received: 30 July 2019; Accepted: 04 September 2019.

et al. (2015); He, Qi, Jiang et al. (2015); Joseph (1988); Li (2009); Michael (2009); Qian (2008); Van (2006); Wang (2018); Xiao and Jun (2009)], is a great challenging problem. Confronting with challenges and high requirement of the reentry attitude control, many researchers have made great effort, and various control schemes have been provided.

The gain-scheduling control approach is one of the classical and effective approaches [Roenneke and Markl (1994)], but the limitation is that a large number of control gains to be designed and scheduled in the HSV attitude controller. The feedback linearization [Balas, Reiner and Garrard (1996)] and dynamic inversion [Bharadwaj, Rao and Mease (1998)] methods are alternate control approaches whereas the exact model of the HSV is needed for controller synthesis. Moreover, the sliding mode control (SMC) [Sagliano, Mooij and Theil (2017)] is a popular technique for handling the uncertainties and unknown external disturbances, which can derive the sliding variables into origin in finite time by discontinuous injection [Edwards and Spurgeon (1998)]. However, the uncertainties existing in the HSV attitude system may not satisfy the matching condition [Xu, Mirmirani and Ioannou (2004)].

The disturbance observer-based control method has been received much attention in the past few years [Chen, Ohnishi and Guo (2015); Tian, Liu, Lu et al. (2018)]. It has been extensively applied in the HSV control system [Li and Yang (2013); Yang, Li and Sun (2013)]. The idea of the method is to design a disturbance observer which is used to estimate external disturbances and plant uncertainties. Then, the disturbance observer-based compensation is added to improve the robustness and disturbance attenuation with a baseline controller.

More recently, a new continuous output feedback multivariable uniform finite-time reentry attitude control scheme is developed for HSV with matched and mismatched disturbances in Chen et al. [Chen, Yang, Guo et al. (2016); Li, Zhou and Yu (2013); Mohammadi, Tavakoli, Marquez et al. (2013); Tian, Lu, Zuo et al. (2018)]. The uniform finite-time convergent controller and observer are designed using the bi-limit homogeneous and the sliding mode differentiator technique, respectively. The aeroservoelastic model of HSV is established by using hypothetical modal method and Galerkin method in Mao et al. [Mao, Dou, Tian et al. (2018)], and a novel reentry attitude control scheme via Type-2 AFSMC method is proposed that achieves stable and reliable reentry flight with aeroservoelastic effect. Furthermore, a novel actuator fault-tolerant control scheme for reentry hypersonic vehicle is equipped with aerodynamic surfaces and reaction control systems (RCS) in Zhai [Zhai (2019)], and a nonlinear disturbance observer based sliding mode controller is designed to calculate the required attitude control torque which can handle system uncertainties and external disturbances together.

The model predicative control (MPC) approach is one of effective approaches to deal with model uncertainty and external unknown disturbances, and also provide the optimal tracking performance. The basic idea is to employ the system model to predict future states of the systems. State predictions are then used to determine future control moves while minimizing future errors and control effort [Cheng, Tang, Wang et al. (2015); Edwards and Spurgeon (1998); Sagliano, Mooij and Theil (2017); Xiao and Jun (2009);]. As we know, there is no existing research work on the model predicative control study on the reentry control problem considering the coupling of RCS and aerodynamic

surfaces. Therefore, this paper focuses on the model predictive control problem of HSV with equipped with both RCS and aerodynamic surfaces.

The rest of article is organized as follows: Section 1 introduces the attitude dynamical model of the hypersonic vehicles in reentry phase, and the dynamic characteristics in the wide flight envelope is analyzed. Section 2 presents the compound control allocation strategy and the model predictive controller design method for the pitch channel is proposed, and an improved model predictive control (IMPC) approach is presented by introducing the online parameter estimation of the jet interaction coefficient for dealing with the uncertainty and disturbance. In Section 3, considering the strong coupling effect between the yaw channel and roll channel, a coupled model predictive controller is designed by introducing the feedback of sideslip angle into the roll control channel to eliminate the coupling effect. Several representative simulations are conducted in Section 4. Finally, Section 5 concludes this paper briefly.

2 Attitude dynamic model of HSV

2.1 Nonlinear dynamic model

Considering the reentry phase from suborbit to atmosphere, the HSV is controlled by the RCS and aerodynamic surfaces together. The attitude dynamic model of the HSV in the reentry phase is as follows:

$$\begin{cases} \dfrac{d\omega_x}{dt} = \dfrac{\left(J_y - J_z\right)}{J_x}\omega_z\omega_y + \dfrac{M_x}{J_x} \\ \dfrac{d\omega_y}{dt} = \dfrac{\left(J_z - J_x\right)}{J_y}\omega_x\omega_z + \dfrac{M_y}{J_y} \\ \dfrac{d\omega_z}{dt} = \dfrac{\left(J_x - J_y\right)}{J_z}\omega_x\omega_y + \dfrac{M_z}{J_z} \end{cases}$$

$$\begin{cases} \dfrac{d\alpha}{dt} = -\omega_x\cos\alpha\tan\beta + \omega_y\sin\alpha\tan\beta + \omega_z - \dfrac{Y}{mV\cos\beta} + \dfrac{g\cos\theta\cos\gamma_V}{V\cos\beta} \\ \dfrac{d\beta}{dt} = \omega_x\sin\alpha + \omega_y\cos\alpha - \dfrac{Z}{mV} + \dfrac{g\cos\theta\sin\gamma_V}{V} \\ \dfrac{d\gamma_V}{dt} = \dfrac{\omega_x\cos\alpha}{\cos\beta} - \dfrac{\omega_y\sin\alpha}{\cos\beta} + \dfrac{Y\left(\tan\beta + \tan\theta\sin\gamma_V\right) + Z\tan\theta\cos\gamma_V}{V} - \dfrac{g\cos\theta\tan\beta\cos\gamma_V}{V} \end{cases} \tag{1}$$

where variables are represented as follows: α, β, γ_V are angle of attack, sideslip angle, and bank angle; $\omega_x, \omega_y, \omega_z$ are bank, pitch, and yaw angular rates; ,Y, Z are lift force and lateral force; M_x, M_y, M_z are bank, yaw and pitch torques; J_x, J_y, J_z are bank, yaw, and pitch torques of inertial; V, m, g, θ are velocity, vehicle mass, gravity acceleration, the flight path angle.

3 MPC-based compound control design

3.1 Compound control strategy

In the reentry phase of HSV, when aerodynamic surfaces cannot provide the required

attitude control torque due to low dynamic pressure, RCS are activated to assist aerodynamic surfaces to generate the residual torque. Therefore, a compound control strategy should be provided at first.

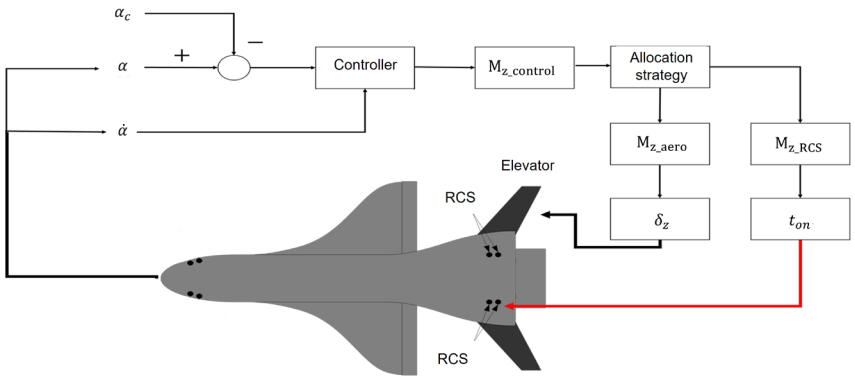

Figure 1: Illustration of compound control strategy

As shown in Fig. 1, the required control torque is firstly generated by the tracking controller to be designed, then a torque allocation strategy is given to distribute the required torque command to RCS and aerodynamic surfaces. Considering the optimization of fuel consumption, the aerodynamic surfaces work as the primary actuators and RCS serves as auxiliary actuators to complement the residual torque.

3.2 Model predictive control design of HSV

The MPC approach is one of effective approaches to deal with model uncertainties and unknown disturbances, and also provide the optimal tracking performance. The basic idea is to employ the system model to predict future states of the systems. State predictions are then used to determine future control moves while minimizing future errors and control effort.

With the help of Taylor's expansion [Cheng, Tang, Wang et al. (2015); Van (2006); Xiao and Jun (2009)], the following longitudinal discrete prediction model can be derived from attitude dynamic model of the HSV.

$$\begin{pmatrix} \alpha(t+h) \\ \alpha(t+2h) \\ \alpha(t+3h) \\ \cdots \\ \alpha(t+nh) \end{pmatrix} = \begin{pmatrix} \alpha(t)+h*\omega_z(t) \\ \alpha(t)+2h*\omega_z(t) \\ \alpha(t)+3h*\omega_z(t) \\ \cdots \\ \alpha(t)+nh*\omega_z(t) \end{pmatrix} + \frac{1}{Jz} \begin{pmatrix} \frac{h^2}{2} & 0 & 0 & \cdots & 0 \\ \frac{3h^2}{2} & \frac{h^2}{2} & 0 & \cdots & 0 \\ \frac{5h^2}{2} & \frac{3h^2}{2} & \frac{h^2}{2} & \cdots & 0 \\ \cdots & \cdots & \cdots & \cdots & 0 \\ \frac{(2n-1)h^2}{2} & \frac{(2n-3)h^2}{2} & \frac{(2n-5)h^2}{2} & \cdots & \frac{h^2}{2} \end{pmatrix} \begin{pmatrix} u(t) \\ u(t+h) \\ u(t+2h) \\ \cdots \\ u(t+nh) \end{pmatrix} \tag{2}$$

The above predictive model can be reformulated as

$$\hat{y}(k) = y_0(k) + bu(k) \tag{3}$$

The following quadratic performance index function is chosen as:

$$J = \sum_{j=1}^{n} \left(\left[\hat{y}(k+j) - y_c(k+j) \right]^2 + Qu(k+j-1)^2 \right) \tag{4}$$

where $\left[\hat{y}(k+j) - y_c(k+j) \right]$ represents the tracking error of the step $k+j$ predicted in the step k, and $u(k+j-1)$ represents the control sequence at step . Q denotes weight coefficient to reflect the importance level of tracking error and consumed control energy, and n denotes the maximum predicted length at one time.

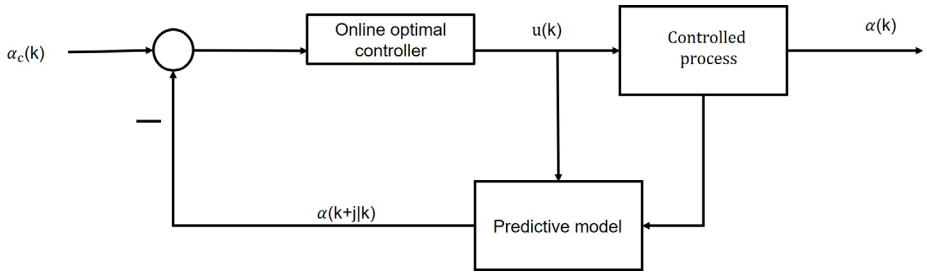

Figure 2: Longitudinal MPC strategy

Considering of the optimization problem of the proposed performance index (4), the required MPC input can be obtained by the minimal principle [Balas, Reiner and Garrard (1996); Xiao and Jun (2009)]:

$$u = (Q * \mathrm{b}^T b + I)^{-1} Q b^T (y_c - \mathrm{y}_0) \tag{5}$$

Here, only the first value of the obtained optimal control input sequence is selected as the control torque required for the HSV at this moment:

$$M_{z\_control} = [1 \quad 0 \quad \cdots \quad 0]u \tag{6}$$

3.3 IMPC via jet interference factor identification

When the RCS is activated, a complicated jet interaction flow field caused by the mixture of the jet and the freestream will bring complicated effect on the control properties of RCS and aerodynamic surfaces. In order to attenuate the effects of the above issues on the control performance of the reentry phase of HSV, an improved model predictive control (IMPC) approach is presented by introducing the online parameter identification of the jet interaction coefficient.

First, the online estimation of the jet interference factor is performed, and it is assumed that the jet interference factor changes slowly [Balas, Reiner and Garrard (1996)]. The jet interference factor K_F in this paper is defined as follows:

$$K_F = \frac{\mathrm{u}_{\mathrm{real}}}{\mathrm{u}_{\mathrm{theory}}} \tag{7}$$

where $\mathrm{u}_{\mathrm{real}}$ is the control torque that the HSV subjected under actual flight conditions, and $\mathrm{u}_{\mathrm{theory}}$ is the control torque calculated by the controller. After adding the effect of jet interference factor, the predictive model can be corrected as:

$$\hat{\mathrm{y}}(k) = y_0(k) + K_F * \mathrm{b}u(k) \tag{8}$$

Considering the slow variation property of K_F, which can be treated as constant in one period. Therefore, the estimated value of K_F can be obtained by the following relationship.

$$K_F = \sum_{i=1}^{k} [y(k-i) - y_0(k-i)] / u(k-i) \tag{9}$$

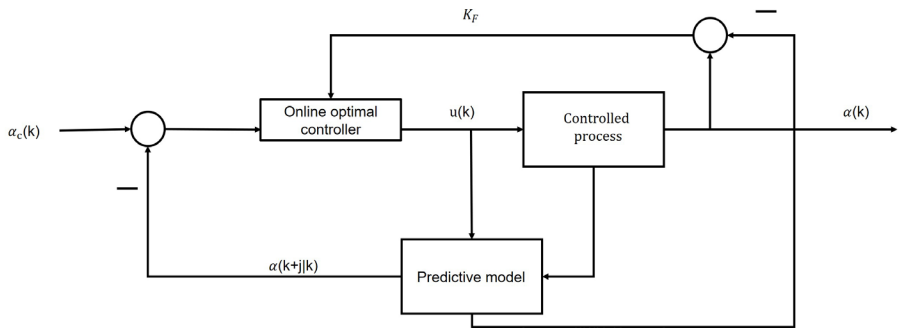

Figure 3: IMPC strategy

By introducing the estimated jet interference factor into the online computation process, the model predictive controller is updated continually. The more accurate predictive dynamic result is, the better control performance will be achieved.

3.4 Pulse amplitude modulation

It can be found that the control torque is designed in the continuous torques, but RCS of HSV have the discrete working mechanism. Motivated on this observation, the following conversion method is proposed using the principle of impulse equivalence.

For given sampling period, the discrete torques are modulated into pulse sequences of different widths and amplitudes. The pulse equivalent principle [Xiao and Jun (2009)] is shown in the figure:

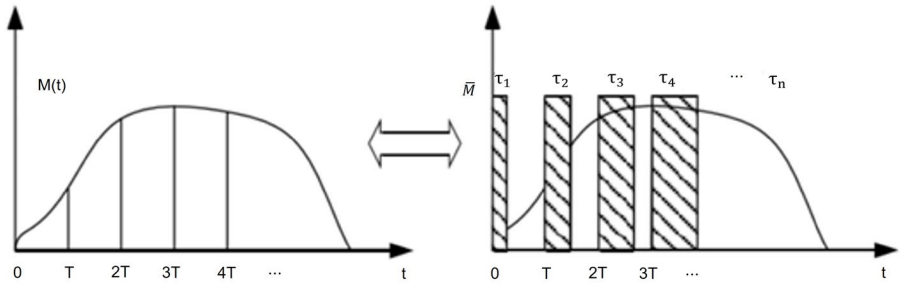

Figure 4: Schematic diagram of pulse equivalence principle

$$M_{rcs} * t_{on} = M_{control} * T \tag{10}$$

Among them, M_{rcs} is the fixed control torque generated by RCS , and t_{on} denotes the period when RCS activating in a sampling period T, and $M_{control}$ is the control torque

required for each sampling period calculated by the controller. The torque allocated to the RCS at this time can be realized by t_{on}.

4 Lateral coupled IMPC design

Considering the strong coupling effect between the yaw channel and roll channel, a coupled model predictive controller is designed by introducing the feedback of sideslip angle into the roll control channel to eliminate the coupling effect. Similar with the longitudinal case, the lateral discretization prediction model of HSV can be obtained via Taylor's expansion [Cheng, Tang, Wang et al. (2015); Xiao and Jun (2009)].

$$\begin{pmatrix} \beta(t+h) \\ \beta(t+2h) \\ \beta(t+3h) \\ \cdots \\ \beta(t+nh) \end{pmatrix} = \begin{pmatrix} \beta(t)-h*\cos(\alpha(t))*\omega_y(t) \\ \beta(t)-2h*\cos(\alpha(t))*\omega_y(t) \\ \beta(t)-3h*\cos(\alpha(t))*\omega_y(t) \\ \cdots \\ \beta(t)-nh*\cos(\alpha(t))*\omega_y(t) \end{pmatrix} + \frac{B_y}{Jy} \begin{pmatrix} u(t) \\ u(t+h) \\ u(t+2h) \\ \cdots \\ u(t+(n-1)h) \end{pmatrix} \tag{11}$$

$$\begin{pmatrix} \gamma_V(t+h) \\ \gamma_V(t+2h) \\ \gamma_V(t+3h) \\ \cdots \\ \gamma_V(t+nh) \end{pmatrix} = \begin{pmatrix} \gamma_V(t)+h*\cos(\alpha(t))*\omega_x(t) \\ \gamma_V(t)+2h*\cos(\alpha(t))*\omega_x(t) \\ \gamma_V(t)+3h*\cos(\alpha(t))*\omega_x(t) \\ \cdots \\ \gamma_V(t)+nh*\cos(\alpha(t))*\omega_x(t) \end{pmatrix} + k_3\beta(t) + \frac{C_x}{Jx} \begin{pmatrix} u(t) \\ u(t+h) \\ u(t+2h) \\ \cdots \\ u(t+(n-1)h) \end{pmatrix}$$

where B_z and C_z are as follows:

$$B_y = \begin{pmatrix} \frac{h^2}{2} & 0 & 0 & \cdots & 0 \\ \frac{h^2}{2}-h^2*\cos(\alpha(t)) & \frac{h^2}{2} & 0 & \cdots & 0 \\ \frac{h^2}{2}-2h^2*\cos(\alpha(t)) & \frac{h^2}{2}-h^2*\cos(\alpha(t)) & \frac{h^2}{2} & \cdots & 0 \\ \cdots & \cdots & \cdots & \cdots & 0 \\ \frac{h^2}{2}-(n-1)h^2*\cos(\alpha(t)) & \frac{h^2}{2}-(n-2)h^2*\cos(\alpha(t)) & \cdots & \cdots & \frac{h^2}{2} \end{pmatrix}$$

$$C_x = \begin{pmatrix} \frac{h^2}{2} & 0 & 0 & \cdots & 0 \\ \frac{h^2}{2}+h^2*\cos(\alpha(t)) & \frac{h^2}{2} & 0 & \cdots & 0 \\ \frac{h^2}{2}+2h^2*\cos(\alpha(t)) & \frac{h^2}{2}+h^2*\cos(\alpha(t)) & \frac{h^2}{2} & \cdots & 0 \\ \cdots & \cdots & \cdots & \cdots & 0 \\ \frac{h^2}{2}+(n-1)h^2*\cos(\alpha(t)) & \frac{h^2}{2}+(n-2)h^2*\cos(\alpha(t)) & \cdots & \cdots & \frac{h^2}{2} \end{pmatrix} \tag{12}$$

The above predictive model can be reformulated as

$$\begin{aligned} \hat{y}_1(k) &= \mathrm{y1}_0(k) + \mathrm{b}_1 u_1(k) \\ \hat{y}_2(k) &= \mathrm{y2}_0(k) + \mathrm{b}_2 u_2(k) \end{aligned} \tag{13}$$

The following quadratic performance index functions are chosen as:

$$J_1 = \sum_{j=1}^{n}\left(\left[\hat{y}_1(k+j) - y1_c(k+j)\right]^2 + Q_1 u_1(k+j-1)^2\right)$$
$$J_2 = \sum_{j=1}^{n}\left(\left[\hat{y}_2(k+j) - y2_c(k+j)\right]^2 + Q_2 u_2(k+j-1)^2\right) \tag{14}$$

where $\left[\hat{y}_1(k+j) - y1_c(k+j)\right]$ and $\left[\hat{y}_2(k+j) - y2_c(k+j)\right]$ represent the tracking error of the step $k+j$ predicted in the step k in yaw and roll channel. $u_1(k+j-1)$ and $u_2(k+j-1)$ represent the control sequence at step in yaw and roll channel. Q_1 and Q_2 denote weight coefficient to reflect the importance level of tracking error and consumed control energy in yaw and roll channel, and n denotes the maximum predicted length at one time.

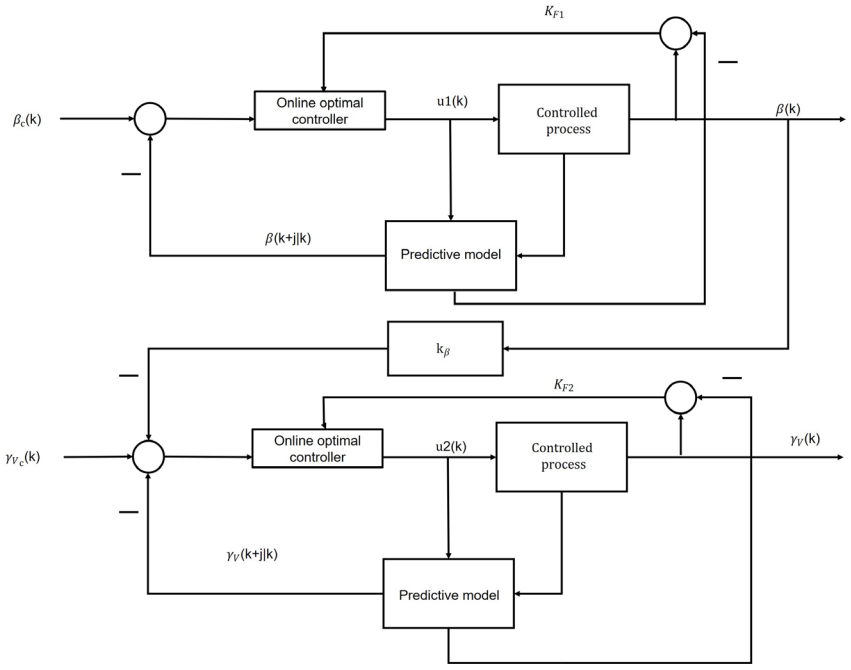

Figure 5: Lateral coupled IMPC strategy

where k_β is the coefficient of introducing side slip angle negative feedback to eliminate serious lateral coupling effect, and K_{F1}, K_{F2} are the jet interference factors of yaw and roll channel. Considering of the optimization problem of the proposed performance index (23), the required MPC input can be obtained by the minimal principle:

$$u_1 = (Q_1 * \mathrm{b}_1^T b_1 + I)^{-1} Q_1 b_1^T (y1_c - \mathrm{y1}_0)$$
$$u_2 = (Q_2 * \mathrm{b}_2^T b_2 + I)^{-1} Q_2 b_2^T (y2_c - \mathrm{y2}_0) \tag{15}$$

Here, only the first value of the obtained optimal control input sequence is selected as the control torque required for the HSV at this moment:

$$M_{\mathrm{y}\_control} = [1 \quad 0 \quad \cdots \quad 0]u_1$$
$$M_{x\_control} = [1 \quad 0 \quad \cdots \quad 0]u_2 \tag{16}$$

5 Simulation results

5.1 Simulation input

To verify the effectiveness of the proposed method, the simulations are carried out. The dynamic parameters of HSV are given as following table.

Table 1: Input parameters

Roll torque of inertia	J_x	11810 kg.m^2
Yaw torque of inertia	J_y	209300 kg.m^2
Pitch torque of inertia	J_z	203050 kg.m^2
Mass	M	8000 kg
Reference area	S	0.415 m^2
Gravity acceleration	g	9.8065 m/s^2
Prediction model steps	n	5
K_F Identification model steps	k	5
Roll torque of RCS	Mx_{rcs}	1929 N.m
Yaw torque of RCS	My_{rcs}	3857 N.m
Pitch torque of RCS	Mz_{rcs}	7714 N.m

5.2 Simulation results

In order to verify the robustness of the proposed control strategy, the aerodynamic coefficients are assumed to remain within the 20% uncertainty about the nominal value, the simulation results in this paper are as follows.

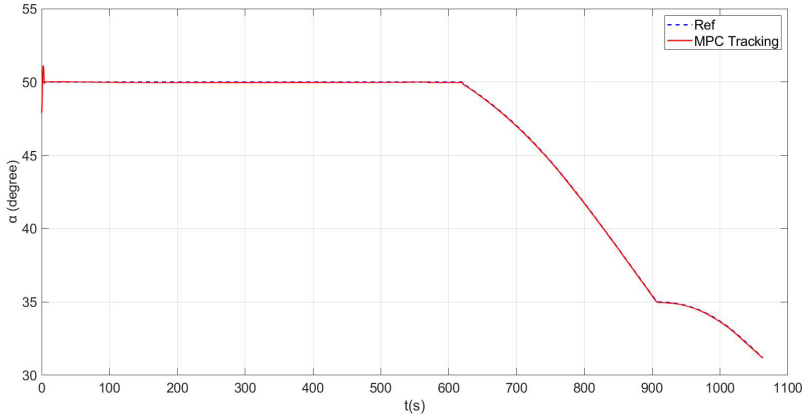

Figure 6: Time histories of the angle of attack

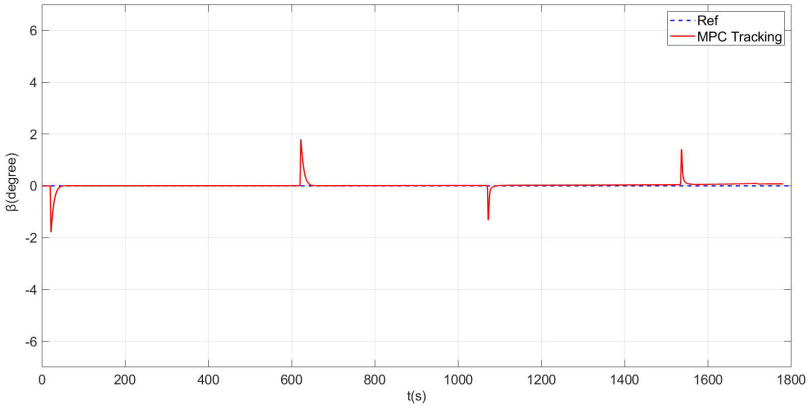

Figure 7: Time histories of the sideslip angle

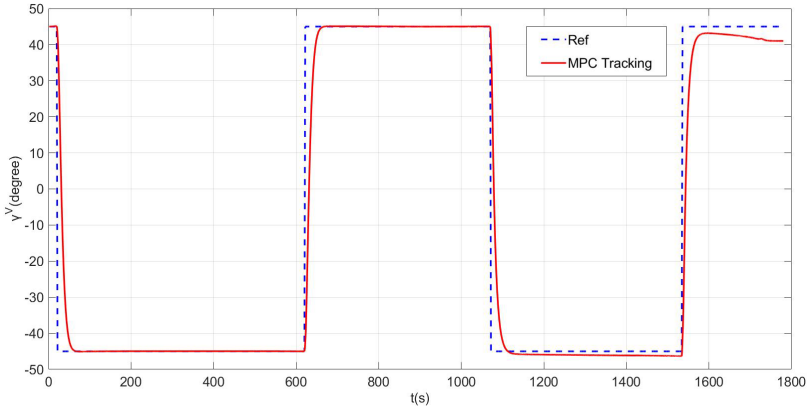

Figure 8: Time histories of the bank angle

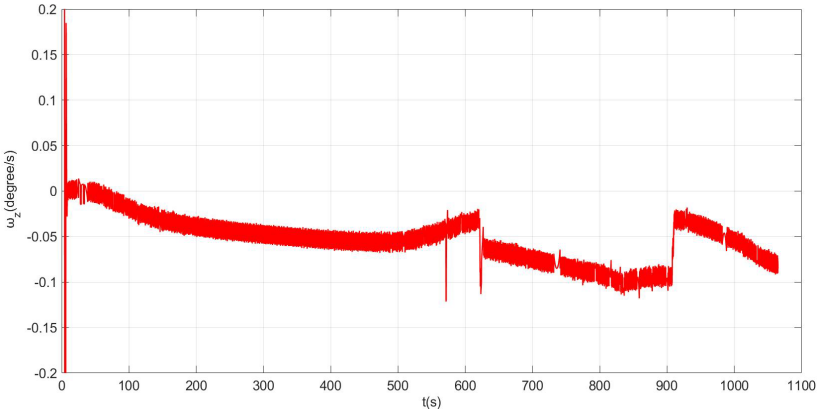

Figure 9: Time histories of the pitch angle rate

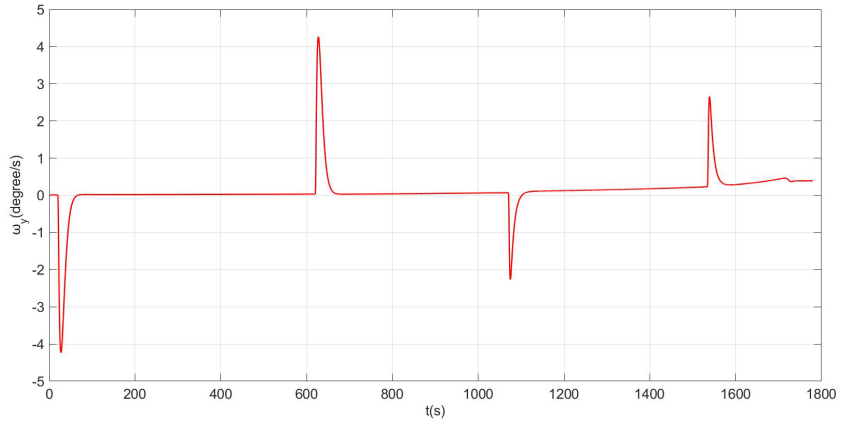

Figure 10: Time histories of the sideslip angle rate

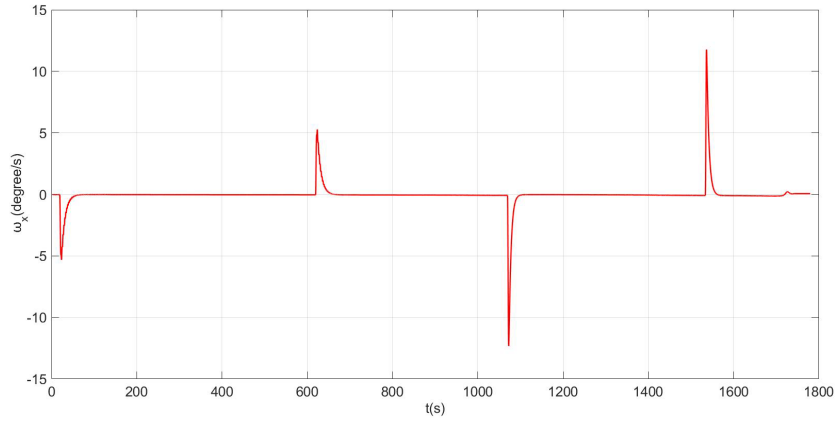

Figure 11: Time histories of bank angle rate

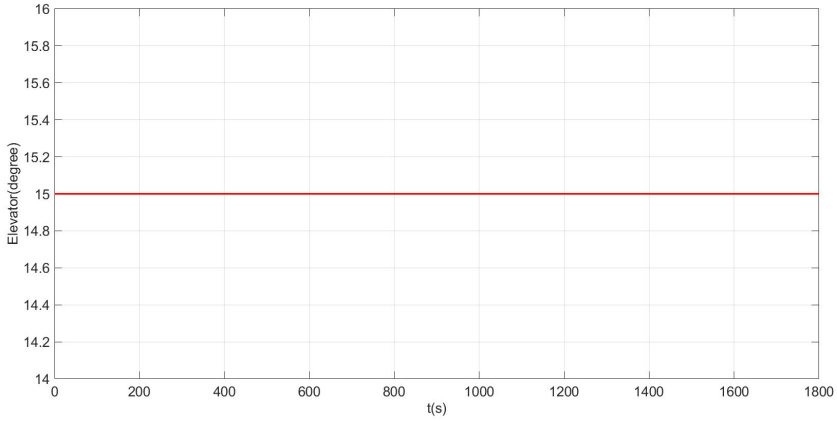

Figure 12: Time histories of the elevator deflection

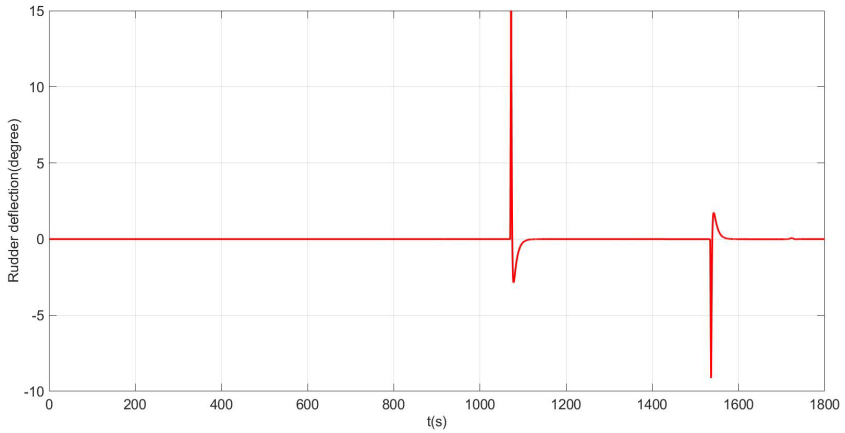

Figure 13: Time histories of the rudder deflection

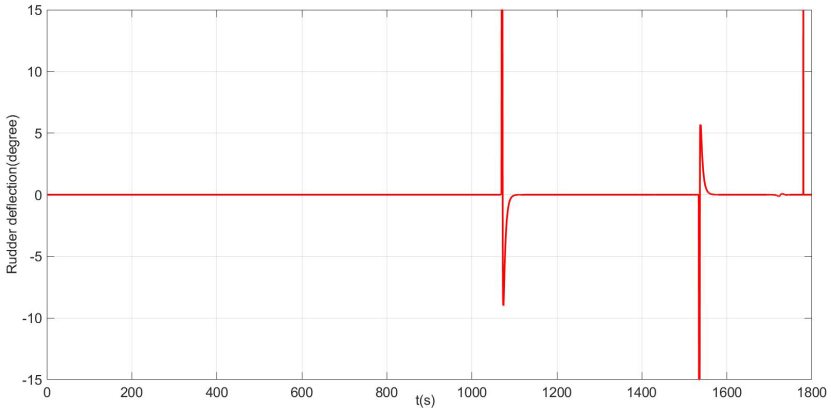

Figure 14: Time histories of the aileron deflection

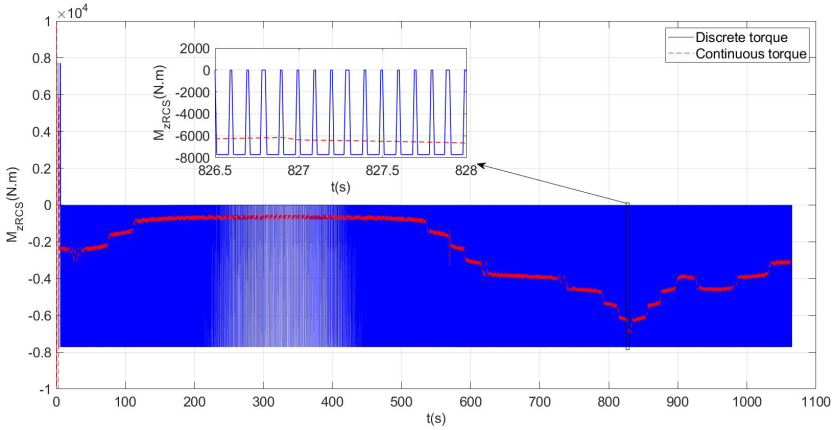

Figure 15: Time histories of the RCS torque in pitch channel

The results demonstrate the tracking accuracy and robustness of the MPC approach and control allocation algorithm. Particularly, from Fig. 15, it shows the effectiveness of RCS pulse amplitude modulation, where RCS activates only in parts of sample time.

5.3 Comparative analysis

5.3.1 Comparison of MPC and PID control approach

Employing the designed MPC and PID controller, the comparative simulations are carried out with the same initial condition, the results are as below.

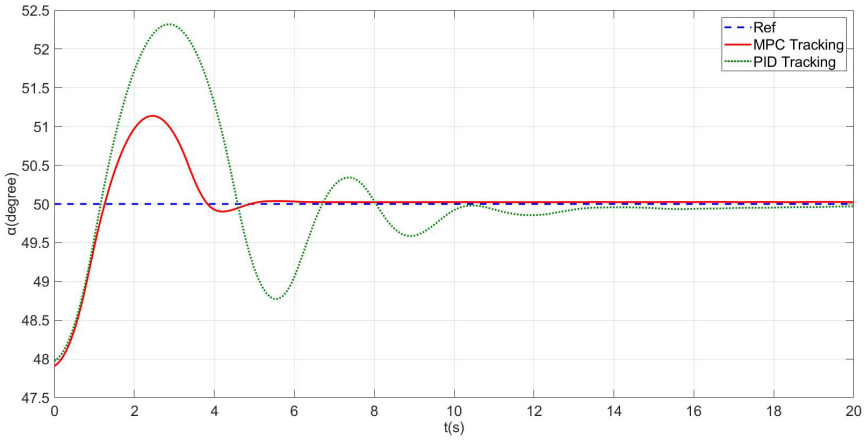

Figure 16: MPC *vs.* PID: angle of attack

As shown above, the green dotted line is part of the attitude angle tracking curve of the PID. The blue dashed line is the reference value and the red solid line is the attitude angle tracking curve of the MPC. It can be found that compared with the traditional PID control approach, the response speed of the MPC approach is faster, which means better control performance in the reentry phase.

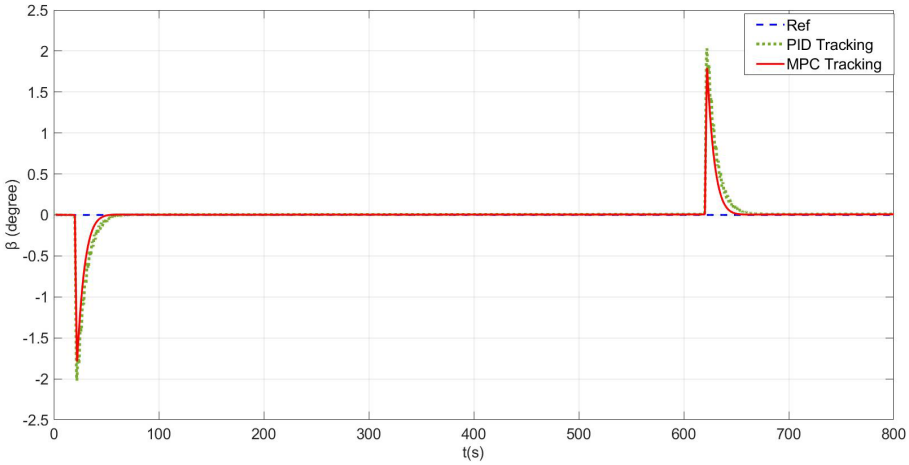

Figure 17: MPC *vs.* PID: sideslip angle

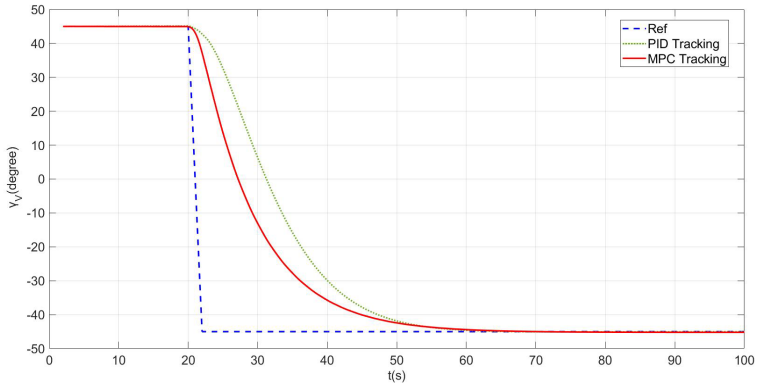

Figure 18: MPC *vs.* PID: bank angle (Partial time histories)

5.3.2 Comparison of MPC and IMPC

The MPC and IMPC approaches are employed for the attitude control design respectively, and the comparative simulations are carried out with the same initial condition, the results are as below.

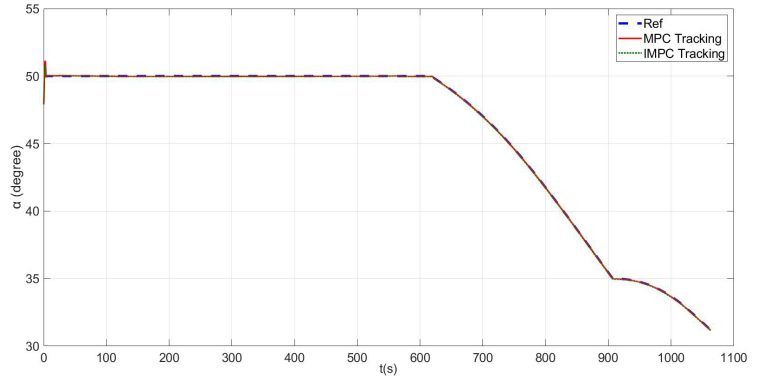

Figure 19: MPC *vs.* IMPC: angle of attack

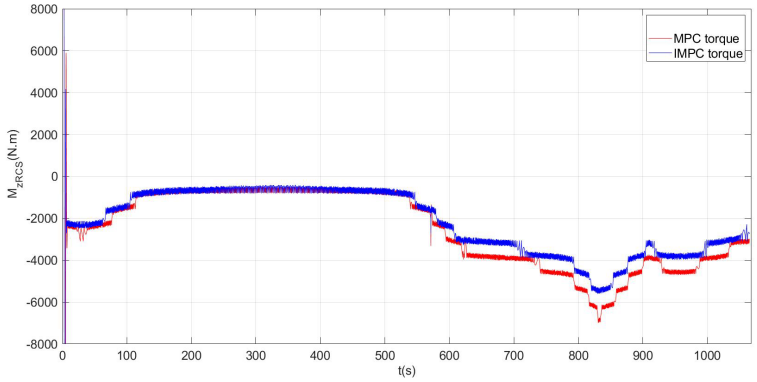

Figure 20: MPC and IMPC: required pitch torque

Although it can be seen from Fig. 19 that both of MPC and IMPC have good tracking performance, the MPC approach require larger torque comparing with IMPC approach, which illustrates the advantage of IMPC by introducing the identification of jet interference factor.

5.3.3 Comparison of decoupled control and coupled control approach

The decoupled control and coupled control approaches are employed for the lateral attitude control design respectively, and the comparative simulations are carried out with the same initial condition, the results are as below.

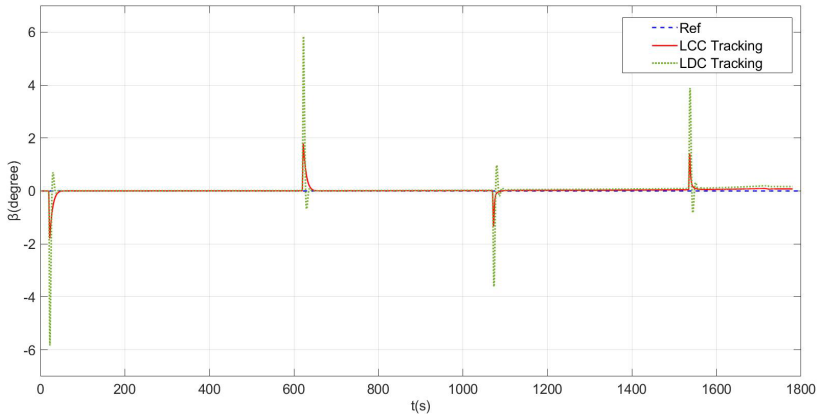

Figure 21: Time histories of the sideslip angle

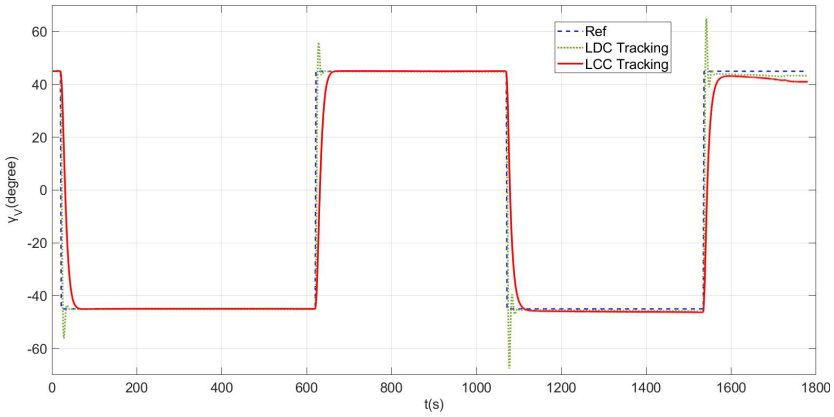

Figure 22: Time histories of the bank angle

As shown above, the green dotted line is the sideslip angle and the bank angle tracking curve based on lateral decoupled control (LDC). The blue dashed line is the reference value and the red solid line is the sideslip angle and the bank angle tracking curve based on lateral coupled control (LCC). It can be seen that compared with the decoupled control; the coupled control approach has less overshot when reference bank angle reverses sign, which means the better control performance.

6 Conclusion

Aiming at the reentry attitude control problem of HSV with reaction control systems (RCS) and aerodynamic surfaces, this paper provides a novel model predictive control approach to cope with the dynamic uncertainty and coupling effect. On one hand, considering the jet interaction effect of HSV during RCS working, an improved model predictive (IMPC) control approach is proposed by introducing the online parameter estimation of the jet interaction coefficient for dealing with the uncertainty and disturbance; On the other hand, considering the strong coupling effect between the yaw channel and roll channel, a coupled model predictive controller is designed by introducing the feedback of sideslip angle into the roll control channel to eliminating the coupling effect. Especially, the comparison simulations results demonstrate the effectiveness and efficiency of the proposed approach.

Acknowledgment: This work is supported by National Natural Science Foundation of China under grants NSFC 61603363, 61703383, 61603056.

Conflicts of Interest: The authors declare that they have no conflicts of interest to report regarding the present study.

References

Balas, G. J.; Reiner, J.; Garrard, L. W. (1996): Flight control design using robust dynamic inversion and time-scale separation. *Automatic*, vol. 32, no. 11, pp. 1493-1504.

Bharadwaj, S.; Rao, A. V.; Mease, K. D. (1998): Entry trajectory tracking law via feedback linearization. *Journal of Guidance Control and Dynamics*, vol. 21, no. 5, pp. 726-732.

Chen, W. H.; Ohnishi, K.; Guo, L. (2015): Advances in disturbance/uncertainty estimation and attenuation. *IEEE Transactions on Industrial Electronics*, vol. 62, no. 9, pp. 5758-5762.

Chen, W. H.; Yang, J.; Guo, L.; Li, S. H. (2016): Disturbance-observer-based control and related methods-An overview. *IEEE Transactions on Industrial Electronics*, vol. 63, no. 2, pp. 1083-1095.

Cheng, X. L.; Tang, G. J.; Wang, P.; Liu, L. H. (2015): Predictive sliding mode control for attitude tracking of hypersonic vehicles using fuzzy disturbance observer. *Mathematical Problems in Engineering*, vol. 2015, pp. 1-13.

Edwards, C.; Spurgeon, S. K. (1998): *Sliding Mode Control: Theory and Applications*. CRC Press.

Feng, Z. J.; Zhou, J. (2017): Design of multi-constrained robust attitude controller for hypersonic vehicle. *Journal of Astronautics*, vol. 38, no. 8, pp. 839-846.

Greg, J. G. (2006): Cost comparison of expendable hybrid and reusable launch vehicles. *Air Force Institute of Technology Air University*, vol. 7211, pp. 19-21.

Guo, Z. Y.; Zhou, J.; Guo, J. G.; Cieslak, J.; Chang, J. (2017): Coupling characterization-based robust attitude control scheme for hypersonic vehicles. *IEEE Transactions on Industrial Electronics*, vol. 64, no. 8, pp. 50-61.

He, J.; Qi, R.; Jiang, B.; Qian, J. (2015): Adaptive output feedback fault-tolerant control design for hypersonic flight vehicles. *Journal of the Franklin Institute*, vol. 352, no. 5, pp. 1811-1835.

Joseph, A. P. (1988): Application of linear programming to coordinated management of jets and aerosurfaces for aerospace vehicle control. *Journal of Guidance, Control and Dynamics*, vol. 14, no. 1, pp. 44-50.

Li, Q. Q. (2009): Dynamic modeling and simulation of reentry segment of hypersonic vehicle. *Journal of System Simulation*, vol. 21, no. 2, pp. 534-537.

Li, S. H.; Yang, J. (2013): Robust autopilot design for bank-to-turn missiles using disturbance observers. *IEEE Transactions on Aerospace and Electronic Systems*, vol. 49, no. 1, pp. 558-579.

Li, S. H.; Zhou, M. M.; Yu, X. H. (2013): Design and implementation of terminal sliding mode control method for PMSM speed regulation system. *IEEE Transactions on Industrial Informatics*, vol. 9, no. 4, pp. 1879-1891.

Liu, Q. J. (2011): *Research on Attitude Control Technology of Reentry Stage of Hypersonic Vehicle (Ph.D. Thesis)*. Nanjing University, China.

Mao, Q.; Dou, L. Q.; Tian, B. L.; Zong, Q. (2018): Reentry attitude control for a reusable launch vehicle with aeroservoelastic model using type-2 adaptive fuzzy sliding mode control. *International Journal of Robust and Nonlinear Control*, vol. 2018, pp. 1-18.

Michael, A. B. (2009): Nonlinear robust adaptive control of flexible airbreathing hypersonic vehicles. *Journal of Guidance*, vol. 32, no. 2, pp. 402-416.

Mohammadi, A.; Tavakoli, M.; Marquez, H. J.; Hashemzadeh, F. (2013): Nonlinear disturbance observer design for robotic manipulators. *Control Engineering Practice*, vol. 21, no. 3, pp. 253-267.

Qian, C. S. (2008): Research on reentry mathematical modeling of aerospace aircraft design. *Journal of Astronautics*, vol. 29, pp. 434-439.

Roenneke, A. J.; Markl, A. (1994): Reentry control to a drag-vs-energy profile. *Journal of Guidance Control and Dynamics*, vol. 17, no. 5, pp. 916-920.

Sagliano, M.; Mooij, E.; Theil, S. (2017): Adaptive disturbance-based high-order sliding-mode control for hypersonic-entry vehicles. *Journal of Guidance Control and Dynamics*, vol. 40, no. 3, pp. 521-535.

Tian, B. L.; Liu, L. H.; Lu, H. C.; Zuo, Z. Y.; Zong, Q. et al. (2018): Multivariable finite time attitude control for quadrotor UAV: theory and experimentation. *IEEE Transactions on Industrial Electronics*, vol. 65, no. 3, pp. 2567-2577.

Tian, B. L.; Lu, H. C.; Zuo, Z. Y.; Zong, Q. (2018): Multivariable uniform finite-time output feedback reentry attitude control for RLV with mismatched disturbance. *Journal of the Franklin Institute*, vol. 355, no. 8, pp. 3470-3487.

Van, W. R. (2006): Combined feedback linearization and constrained model predictive control for entry flight. *Journal of Guidance Control and Dynamics*, vol. 29, no. 2, pp. 427-434.

Wang, T. (2018): Reentry vehicle optimal control allocation method using PWPF regulator. *Journal of National University of Defense Technology*, vol. 40, no. 4, pp. 74-79.

Weingarten, S. S. (1993): The reference concept of the germen hypersonic technology program. *AIAA/DGLR 5th International Aerospace Planes and Hypersonic Technologies Conference*, vol. 5022, no. 92.

Xiao, W. S.; Jun, Z. (2009): Nonlinear predictive attitude control of hypersonic vehicle. *Journal of Ballistics*, vol. 21, no. 4, pp. 42-46.

Xu, H. J.; Mirmirani, M. D.; Ioannou, P. A. (2004): Adaptive sliding mode control design for a hypersonic flight vehicle. *Journal of Guidance Control and Dynamics*, vol. 27, no. 5, pp. 829-838.

Yang, J.; Li, S. H.; Sun, C. Y. (2013): Nonlinear-disturbance-observer-based robust flight control for airbreathing hypersonic vehicles. *IEEE Transactions on Aerospace and Electronic Systems*, vol. 49, no. 2, pp. 1263-1275.

Yang, J.; Li, S. H.; Yu, X. H. (2013): Sliding-mode control for systems with mismatched uncertainties via a disturbance observer. *IEEE Transactions on Industrial Electronics*, vol. 60, no. 1, pp. 160-169.

Zhai, R. Y. (2019): Compound fault-tolerant attitude control for hypersonic vehicle with reaction control systems in reentry phase. *ISA Transactions*, vol. 1, pp. 1-5.

Zhou, J.; Liu, K.; She, W. X. (2015): Preliminary analysis for a two-stage-to-orbit reusable launch vehicle. *20th AIAA International Space Plane and Hypersonic Systems and Technologies Conference*, pp. 1-21.